conductivity of 10^7 S/m. Stability conditions for varying amplitudes of the excitation are shown in Table IV. Some of the entries in the $\Delta y/(v_{\max}\Delta t)$ column are less than 1 since $v_{\max}$ is computed with $\mu_{\min}$ while $\lambda_{\min}$ is computed from $\mu_{\max}$. Comparing Tables III and IV it is clear that both the high conductivity and the nonlinearity of the magnetic material contribute to the necessity of reducing the time-step size below the Courant limit.

V. Conclusions

Application of FDTD to a material with both high conductivity and nonlinear magnetic characteristics has been demonstrated. In order to obtain stability, the current density term in the FDTD equation must be calculated from the most recent electric field value, and the time step must be reduced well below the Courant limit. The effects of the high conductivity and nonlinearity of the magnetic material on the time step were investigated, with the result that both parameters affect the time-step size but that the nonlinearity is the more important, especially at relatively large field amplitudes. With the time step reduced sufficiently, FDTD provided extremely accurate results for transient transmission through a highly conductive nonlinear magnetic sheet as compared with previously published results.

References

[1] K. S. Yee, "Numerical solution of initial boundary value problems involving Maxwell's equations in isotropic media," *IEEE Trans. Antennas Propagat.*, vol. AP-14, pp. 302–307, May 1966.

[2] D. E. Merewether, "Electromagnetic pulse transmission through a thin sheet of saturable ferromagnetic material of infinite surface area," *IEEE Trans. Electromagn. Compat.*, vol. EMC-11, pp. 139–143, Nov. 1969.

[3] R. Luebbers, F. Hunsberger, K. Kunz, and R. Standler, "A frequency-dependent finite difference time domain formulation for dispersive materials," *IEEE Trans. Electromagn. Compat.*, Aug. 1990.

[4] ——, "A frequency-dependent time domain formulation for transient propagation in plasma," *IEEE Trans. Antennas Propagat.*, vol. 39, pp. 29–34, Jan. 1991.

[5] J. C. Strikwerda, *Finite Difference Schemes and Partial Differential Equations.* Pacific Grove, CA: Wadsworth & Brooks/Cole, p. 74.

Correction Factor for Nonplanar Incident Field in Monopole Calibrations

J. Randa

***Abstract*—In calibrating monopole antennas, the length of the antenna can be comparable to the separation distance. In that case, there is a significant variation in both the magnitude and the phase of the incident field along the length of the antenna under test. This paper presents an expression for a correction factor to account for this effect. We evaluate the correction factor for some representative cases and present some guidelines for when this factor should be taken into account. The effect can exceed 1 dB in some practical cases.**

The basic idea of monopole calibrations at the National Institute of Standards and Technology (NIST) on an open-area test site [1] is to use a transmitting monopole to generate a known electromagnetic field at the site of the antenna under test (AUT) and to measure the output of the AUT when it is exposed to this known field. The AUT is supposed to be far enough away from the transmitting antenna that the field incident on the AUT can be treated as a plane wave with constant magnitude and phase along the length of the receiving monopole. If the separation distance is not large enough, the incident field is not constant along the length of the AUT, and this introduces an error into the determination of the antenna factor. We shall call this the "nonplanarity" error. This paper evaluates that error and derives a correction factor to eliminate it. There is also another proximity effect, of course, that of the mutual impedance between the two antennas. We expect that the effect of the mutual impedance would be comparable to the nonplanarity error, with the relative importance of the two depending on the frequency, separation distance, and antenna lengths. We do not treat the mutual interactions in this paper; that effect will be addressed at a later date.

The procedures for monopole calibrations on an open-area test site are given in [1]. A representation of the relevant geometry is given in Fig. 1. The z component of the electric field produced by the transmitting antenna at a distance d from the antenna at a height z above the ground plane is given by [2]

$$\begin{aligned} E_z(d,z) &= -j\frac{30I_0^T}{\sin \beta h_T} \cdot \left(\frac{e^{-j\beta r_1}}{r_1} + \frac{e^{-j\beta r_2}}{r_2} - 2\cos \beta h_T \frac{e^{-j\beta r_0}}{r_0}\right) \\ r_0 &= \sqrt{d^2 + z^2} \\ r_1 &= \sqrt{d^2 + (h_T - z)^2} \\ r_2 &= \sqrt{d^2 + (h_T + z)^2} \end{aligned} \tag{1}$$

where β is the wave number, h_T is the height of the transmitting antenna, and we have assumed a sinusoidal current distribution, $I^T(z) = I_0^T \sin[\beta(h_T - z)]/\sin(\beta h_T)$, where I_0^T is the terminal or base current of the transmitting antenna. The open-circuit voltage at the base of the receiving monopole is given by [2]

$$V_{oc}^R = -\frac{1}{I^R(0)} \int_0^{h_R} E_z^{\text{inc}}(z) I^R(z)\, dz \tag{2}$$

where $I^R(z)$ is the current distribution in the receiving antenna, and h_R is its height. Assuming a sinusoidal current distribution and using (1), we obtain

$$V_{oc}^R = j\frac{30I_0^T}{\sin \beta h_T \sin \beta h_R} \int_0^{h_R} \left(\frac{e^{-j\beta r_1}}{r_1} + \frac{e^{-j\beta r_2}}{r_2} - 2\cos \beta h_T \frac{e^{-j\beta r_0}}{r_0}\right) \sin \beta(h_R - z) dz. \tag{3}$$

For large distance (h_T/d and h_R/d small) the incident field is approximately constant, and V_{oc}^R then reduces to

$$V_{oc}^R \approx -E_z^{\text{inc}} \left(\frac{1}{\beta} \tan \frac{\beta h_R}{2}\right) = -E_z^{\text{inc}} h_{\text{eff}}^{th}, \tag{4}$$

where h_{eff}^{th} is the effective length calculated for a sinusoidal current distribution. The central question for present purposes is the difference between (3) and (4) and how that difference affects the antenna factor calculated for the AUT.

Manuscript received January 3, 1992; revised September 2, 1992.

The author is with the Electromagnetic Fields Division, National Institute of Standards and Technology, Boulder, CO 80303.

IEEE Log Number 9204754.

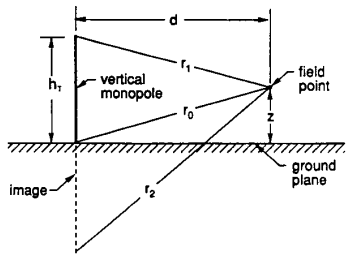

Fig. 1. Geometry of test setup for monopole calibrations.

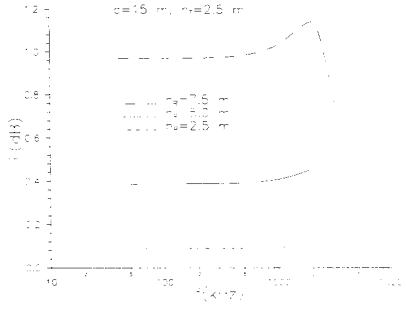

Fig. 2. Frequency dependence of correction factor for $d = 15$ m.

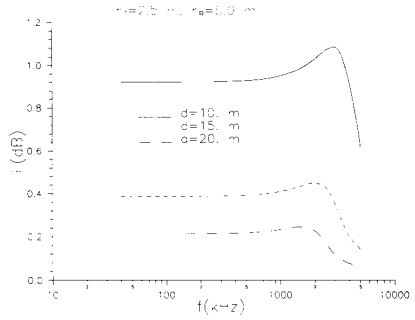

Fig. 3. Frequency dependence of correction factor for $h_R = 5$ m.

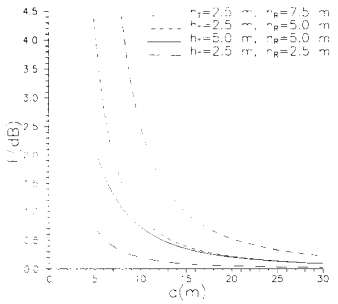

Fig. 4. Correction factor in plateau region as a function of separation distance.

For a uniform incident field E_z^{inc}, the measured antenna factor (K) is obtained from

$$K = \left| \frac{E_z^{\text{inc}}}{V_{50}} \right|, \qquad V_{50} = \frac{V_{oc}^R}{1 + \dfrac{Z_{\text{ant}}}{50}} \tag{5}$$

where V_{50} is the measured voltage into a 50 Ω load, Z_{ant} is the receiving antenna's impedance in ohms. We will not need the value for Z_{ant} since it will not enter into the effect we calculate. Equation (5) assumes a constant incident field E_z^{inc} along the length of the antenna. To relate the quantities measured at finite separation to what would be measured under the idealized conditions assumed in (5), we define a correction factor

$$F \equiv \left| \frac{V_{oc}^R(d)}{V_{oc}^R(\infty)} \right| = \left| \frac{\beta V_{oc}^R(d)}{\tan\left(\frac{\beta h_R}{2}\right) E_z^{\text{inc}}} \right| \tag{6}$$

with $V_{oc}^R(d)$ given by (3) and $V_{oc}^R(\infty)$ given by (4). The true antenna factor is then obtained from the measurements by

$$K = F \left| \frac{E_z^{\text{inc}}}{V_{50}(\text{meas})} \right| \tag{7}$$

where V_{50} (meas) is the measured received voltage, and F is calculated from (6). Since E_z^{inc} varies along the length of the AUT, there is some ambiguity about where E_z^{inc} should be evaluated in (6) or (7). It is important to note, however, that the E_z^{inc} cancels in the expression for the antenna factor, (7), and therefore the choice of where to evaluate E_z^{inc} does not affect the result for the antenna factor, provided that the correction factor has E_z^{inc} evaluated at the same point as it is in the antenna factor, (7). In NIST calibrations, it is evaluated half-way up the monopole, $z = h_R/2$. Choice of a different point at which to evaluate E_z^{inc} would change the value of the correction factor, but it would also change the value of E_z^{inc} in (7), leaving the (corrected) antenna factor unchanged. Using V_{oc}^R from (3) and $E_z^{\text{inc}} = E_z(z = h_R/2)$ from (1), we can then evaluate the correction factor given by (6). (The integral in (3) can be evaluated by standard numerical methods, such as the Romberg routine of [3].)

Representative results for the correction factor as a function of frequency are shown in Figs. 2 and 3. Fig. 2 plots results for various lengths of the receiving monopole for a fixed separation distance (15 m), whereas in Fig. 3 we have fixed h_R (5 m) and plotted the correction factor for selected distances. As expected, the correction factor is larger for longer receiving monopoles and for smaller separation distances. As a function of frequency the correction factor is constant at low frequency, rises to a small peak as frequency increases, and then falls off quite rapidly. Although we have not proved it analytically, in all our numerical evaluations we have found that the peak (or shoulder) occurs at the frequency for which the free-space wavelength is equal to 10 times the separation distance, $f_{pk} = c/(10d)$, where c is the speed of light. Although it is not shown in the figure, as the frequency approaches the resonant frequency of the transmitting antenna, the correction factor in decibels becomes negative. This just reflects the fact that the weighted average of the incident field along the AUT has become less than its value at $z = h_R/2$. The magnitude of F remains small, however. (We assume that the transmitting antenna is not used at frequencies above its first resonance.)

Since the correction factor is approximately constant over a wide range of frequencies, it is natural to ask how the plateau height (the low-frequency value in Figs. 2 and 3) varies with distance. Fig. 4 plots the correction factor, evaluated at 500 kHz, versus distance for various antenna lengths. From this figure we can infer a pair of useful guidelines. The plateau value of the correction factor is less than 1 dB for separation distances greater than twice the height of the receiving monopole, $d > 2h_R$, and it is less than 0.5 dB for $d \geq 3h_R$. The length of the transmitting monopole has a relatively small effect once $d \geq 2h_R$, as can be seen from the results for two different values of h_T for $h_R = 5$ m in Fig. 4.

How these results are to be used will depend on the accuracy desired in a given measurement. If one adheres to the rule that $d \geq 2h_R$ or $3h_R$, then the error due to nonplanarity will be less than 1 dB or 0.5 dB, respectively, even if the correction factor is ignored. (This assumes that E_z^{inc} in (5) is evaluated at $z = h_R/2$, as was done above.) A better approach is to keep $d \geq 2h_R$ or $3h_R$ and to include the correction factor in the calculation of the antenna factor, (7). That should eliminate virtually all nonplanarity error.

ACKNOWLEDGMENT

The author is grateful to Mark Ma and Dennis Camell for their helpful comments.

REFERENCES

[1] D. G. Camell, E. B. Larsen, J. E. Cruz, and D. A. Hill, "NIST calibration procedure for vertically polarized monopole antennas, 30 kHz to 300 MHz," NIST Technical Note 1347, Jan. 1991.
[2] E. C. Jordan and K. G. Balmain, *Electromagnetic Waves and Radiating Systems.* Englewood Cliffs, NJ: Prentice-Hall, 1968, ch. 14.
[3] W. Press, B. Flannery, S. Teukolsky, and W. Vetterling, *Numerical Recipes.* Cambridge, UK: Cambridge University Press, 1986, ch. 4.

Improvements to an Electromagnetic Near-Field Sensor for Simultaneous Electric and Magnetic Field Measurement

Miles E. G. Upton and Andrew C. Marvin

***Abstract*—A sensor for simultaneous electric and magnetic field measurement has been described by Kanda, which relies upon measuring the voltage across precisely matched loads at opposite sides of a loop antenna. This paper describes a modification to the theory to take account of unmatched loading of the loop. Measured results of wave impedance over a 10–400 MHz range demonstrate the accuracy of the modified theory as well as highlighting a novel calibration technique.**

I. INTRODUCTION

In his 1984 paper [1] and a subsequent 1988 paper [2], Kanda described a sensor for simultaneous electric and magnetic field measurement. This sensor is capable of measuring the polarization ellipses of the field vectors in the near field region, as well as the instantaneous Poynting vector. The sensor uses an electrically small loop terminated with two identical loads at diametrically opposite points. In practice, however, it is difficult and often inconvenient to use precisely matched loads to terminate the loop, especially when the sensor is to be used over a wide frequency band. In this correspondence paper, we will be developing Kanda's original theory to take account of unmatched loop loading. The aim is to develop equations relating electric and magnetic field to the voltages measured across the (unmatched) impedances of the loop.

Experimental data will be presented for the measurement of induction-field transverse wave impedance, comparing results obtained using the modified and unmodified theories. For practical reasons, the loop in free space of the original theory will be substituted by a half-loop above a ground plane, although this does not alter the essence of the modifications. The experimental data will be compared with that from an alternative sensor described in [3], which will establish the accuracy of the technique.

Manuscript received January 14, 1991; revised July 26, 1992. This work was supported by the Government Communication Headquarters, Cheltenham, England.

M. E. G. Upton was with Department of Electronics, University of York, Heslington, York, England. He is now with Cambridge Consultants Limited, Science Park, Cambridge, England.

A. C. Marvin is with the Department of Electronics, University of York, Heslington, York, England.

IEEE Log Number 9204755.

II. MODIFICATION TO KANDA'S THEORY

The mathematical theory of the single loop sensor is covered in [1] for the matched load case, and this can be modified as follows to take account of unmatched loads on the outputs of the loop. Consider the equation given in [1] for the current at any point around a loop loaded at opposite points

$$I(o) = 2\pi b E_0^i u(o) - I(0) Z_L v(o) - I(\pi) Z_L w(o) \tag{1}$$

where o is angular position around the loop, $I(0)$ and $I(\pi)$ are the currents through the two loads, E_0^i is the incident field, b is the loop radius and

$$u(o) = \frac{-j}{\pi Z_0}\left(\frac{f_0}{a_0} + \frac{2 f_1 \cos o}{a_1}\right) \tag{2}$$

$$v(o) = \frac{-j}{\pi Z_0}\left(\frac{1}{a_0} + \frac{2\cos o}{a_1}\right) \tag{3}$$

$$w(o) = \frac{-j}{\pi Z_0}\left(\frac{1}{a_0} - \frac{2\cos o}{a_1}\right). \tag{4}$$

It is assumed in these latter equations that components of the loop current of higher order than 1 are insignificant due to the electrical smallness of the loop. The variable f_0 relates the incident field (E_0^i) to the current induced in the loop by the magnetic field and similarly f_1 relates E_0^i to the current induced by the electric field (see [1] for a fuller explanation). a_0 is related to the input admittance of the loop for magnetic loop current by

$$Y_0 = \frac{-j}{\pi Z_0 a_0} \tag{5}$$

a_1 is related to the admittance for the electric dipole current by

$$Y_1 = \frac{-j2}{\pi Z_0 a_1}. \tag{6}$$

The first term on the right-hand side of (1) is derived from the incident field on the loop, whereas the second two terms are related to the currents flowing through the two load impedances at $o = 0$ and $o = \pi$. Substituting unmatched load impedances (Z_1 and Z_2) in (1) and solving for the currents through the two loads gives

$$I(0) = 2\pi b E_0^i u(0) - I(0) Z_1 v(0) - I(\pi) Z_2 w(0) \tag{7}$$

$$I(\pi) = 2\pi b E_0^i u(\pi) - I(0) Z_1 v(\pi) - I(\pi) Z_2 w(\pi) \tag{8}$$

Adding (7) and (8) and substituting (2)–(6) gives

$$I(0) + I(\pi) = 4\pi b E_0^i f_0 Y_0 - 2I(0) Z_1 Y_0 - 2I(\pi) Z_2 Y_0 \tag{9}$$

$$\Rightarrow 4\pi b E_0^i f_0 = \frac{I(0) + I(\pi)}{Y_0} + 2I(0) Z_1 + 2I(\pi) Z_2. \tag{10}$$